0026-895X/92/020286-08$03.00/0

MOLECULAR PHARMACOLOGY, 42:286-293

Two Binding Sites on Angiotensin-Converting Enzyme: Evidence from Radioligand Binding Studies

ROSE B. PERICH, BRUCE JACKSON, FRASER ROGERSON, FREDERICK A. O. MENDELSOHN, DONNA PAXTON, and COLIN I. JOHNSTON

The University of Melbourne, Department of Medicine, Austin Hospital, Heidelberg, Victoria, Australia 3084

Received March 24, 1992; Accepted April 15, 1992

SUMMARY

Purified angiotensin-converting enzyme (ACE) from rat lung and testis, membrane preparations of ACE from lung, kidney, and testis, and ACE from plasma were used in radioligand binding studies, to seek evidence for two binding sites in ACE of somatic origin, as predicted by molecular biology studies. ^{125}I-Ro 31–8472, a radioiodinated hydroxy derivative of cilazaprilat, and ^{125}I-351A, a radioiodinated *p*-hydroxybenzamidine analogue of lisinopril, were used as radioligands. Autoradiographic study of renal ACE using ^{125}I-Ro 31–8472 or ^{125}I-351A showed the same distribution of radioligand binding across kidney sections and identical radioligand binding for purified lung and testis ACE by Western blot, confirming that the same protein bound both radioligands. Analysis of displacement of ^{125}I-Ro 31–8472 binding from ACE by ACE inhibitors 351A and lisinopril yielded biphasic curves for pulmonary, renal, and plasma ACE and a monophasic curve for ACE from the testis. Analysis by LIGAND suggested two binding sites in ACE from plasma or somatic sources and one binding site in ACE of testicular origin, as predicted by molecular biology studies. Displacement of ^{125}I-351A binding from lung and testis ACE by Ro 31–8472 and 351A was monophasic. LIGAND analysis revealed interaction with a single class of binding sites on lung and testis ACE, in agreement with previous studies using ^{125}I-351A. Equilibrium dissociation constants (K_d) for the carboxyl-terminal (K_{d1}) and amino-terminal (K_{d2}) binding sites of purified ACE, using ^{125}I-Ro 31–8472, were similar for Ro 31–8472 (lung K_{d1}, 65 ± 7 pM; K_{d2}, 175 ± 38 pM) but were clearly different for 351A (lung K_{d1}, 19 ± 2 pM; K_{d2}, 2771 ± 489 pM; $p < 0.01$). Cell membrane-associated somatic ACE and plasma ACE, which is devoid of a carboxyl-terminal hydrophobic anchor region, had similar absolute values and differences in 351A binding affinities at the two ACE binding sites. K_d in testis was 46 ± 6 pM for Ro 31–8472 and 16 ± 3 pM for 351A, corresponding to estimates at the carboxyl-terminal binding site of somatic ACE. The 65–200-fold reduction in 351A binding affinity at the amino binding site may limit the detection of two binding sites on somatic ACE by ^{125}I-351A radioligand binding analysis. Displacement curves for ^{125}I-Ro 31–8472 with a panel of ACE inhibitors varied in slope factor between plasma and somatic ACE (lung Ro 31–8472, 0.82 ± 0.03; 351A, 0.38 ± 0.04; $p < 0.001$) but had slope factors approaching 1 for testicular ACE (Ro 31–8472, 0.93 ± 0.02; 351A, 0.96 ± 0.04). Steric hindrance appeared related to ACE inhibitor side chain length. Differential binding parameters for radioligands and ACE inhibitors at two sites on somatic ACE suggest that this enzyme has two active enzymatic sites, which are selective for different natural substrates, and that the biological effects of ACE inhibitor drugs may vary according to their interactions at each of the two enzymatic sites.

ACE (EC 3.4.15.1) is a zinc-containing dipeptidyl carboxypeptidase that plays a pivotal role in generating the potent vasoactive octapeptide angiotensin II from angiotensin I and in degrading bradykinin (1), as well as hydrolyzing other small peptides (2).

The importance of vascular ACE in cardiovascular homeostasis is supported by the beneficial and extensive use of ACE inhibitors in the treatment of hypertension and heart failure (3). ACE is also found in the reproductive tract, gut, renal tubule, and brain, where its role is not known.

This work was supported by grants from the National Health and Medical Research Council of Australia, the National Heart Foundation of Australia, and the Baxter Extramural Grant Program.

Circulating ACE in plasma is thought to be derived from vascular endothelial sources, such as the pulmonary capillaries, because the reported physicochemical, immunological, and biochemical catalytic properties of ACE from lung and plasma are very similar (4). Testicular ACE, located in the seminiferous tubules (5), is catalytically similar to lung and plasma ACE but is of lower molecular weight. Molecular biology studies predict that ACE exists in two forms (6–9). Vascular endothelial cells and epithelial cells of somatic cell origin express an ACE mRNA of ~5 kilobases, coding for a single ~150-kDa protein with two large homologous sequences (amino and carboxyl), each containing a zinc-binding region and active site. The hydrophobic carboxyl-terminal segment, which is absent in plasma ACE, presumably anchors tissue ACE to the cell membrane (6).

ABBREVIATIONS: ACE, angiotensin-converting enzyme; MES, 2-[*N*-morpholino]ethanesulfonic acid; BSA, bovine serum albumin; CV, coefficient(s) of variation; CPA1, carboxypeptidase A1; CPA2, carboxypeptidase A2.

Testicular ACE, of ~100 kDa, is coded by a ~3-kilobase mRNA that is transcribed from the same gene as ACE of somatic cell origin (8, 9). The protein is predicted to resemble the carboxyl-terminal half of somatic ACE (except for a small unique amino-terminal sequence) and consists of only one of the two homologous domains, containing one putative active site.

We have tested the proposition that ACE has two functional enzymatic binding sites by comparison of radioligand binding studies using ^{125}I-Ro 31–8472 and ^{125}I-351A. Binding characteristics of ACE from rat plasma, lung, and kidney, containing two putative binding sites, have been compared with characteristics of ACE from testis. We also characterized the effects of the cell membrane in association with ACE and of the carboxyl-terminal hydrophobic anchor zone of tissue ACE on ACE inhibitor binding affinity at the binding sites on somatic ACE.

Materials and Methods

Relative ACE enzymatic inhibitor potency. The inhibitory potency of Ro 31–8472 was compared with that of the ACE inhibitors cilazaprilat, lisinopril, enalaprilat, and 351A (see Fig. 1). Increasing concentrations of ACE inhibitor were incubated with a fixed quantity of rat plasma ACE. Enzymatic ACE activity was assessed by the kinetic method of Friedland and Silverstein (10), as modified in our laboratory (11), using the substrate hippuryl-histidyl-leucine. The concentration of drug inhibiting ACE enzymatic activity by 50% (IC_{50}) was estimated.

Preparation of radioligands Ro 31–8472 and 351A. Preparation, purification, and stability of radioiodinated 351A have been previously validated and detailed by Jackson *et al.* (12).

Ro 31–8472 is a derivative of the potent ACE inhibitor cilazaprilat. Ro 31–8472 [9-[1-carboxy-3-(4-hydroxyphenyl)propylamino]-octahydro-10-oxo-6*H*-pyridazo[1,2-9][1,2]diazepine-1-carboxylic acid] was synthesized by Roche (Hertfordshire, London) and kindly provided by Dr. M. R. Attwood. The *p*-nitro-dibutyl ester (Ro 31–4827) was hydrogenated to give the amine diester, which was hydrolyzed to the dicarboxylate. The amine was diazotized and decomposed with boiling sulfuric acid. The product (Ro 31–8472) was recovered from dilute acid solution by using a Sep-Pak C_{18} cartridge (Waters Associates, Milford, MA) and was then purified by reverse phase high performance liquid chromatography.

The purity of Ro 31–8472 was assessed by high performance liquid chromatography on a Novapac C_{18} reverse phase 5-μm column (Waters Associates), equilibrated with 20% acetonitrile and 0.08% trifluoroacetic acid as mobile phase. A 300-μl 20 μM Ro 31–8472 sample in mobile phase was injected at a 1 ml/min flow rate, and absorbance was monitored at 214 nm.

Ro 31–8472 was iodinated by the chloramine T method of Hunter and Greenwood (13). To 380 ng of Ro 31–8472 in 10 μl of distilled water, 20 μl of 0.5 M potassium phosphate buffer, pH 7.5, were added, followed by 10 μl of Na[^{125}I] (1 mCi) and 10 μl of chloramine T (1 mg/ml in 0.1 M potassium phosphate buffer, pH 7.5). The mixture was stirred very gently for 45 sec, and then 10 μl of sodium metabisulfite (5 mg/ml in distilled water) were added and mixed, followed by 250 μl of 0.1 M sodium acetate buffer, pH 4.0. The iodination mixture was loaded onto a 0.9- × 60-cm column of Sephadex G-25 Superfine (Pharmacia, Uppsala, Sweden), equilibrated in 0.1 M sodium acetate buffer, pH 4.0. One-milliliter fractions were collected, with the second radioactive peak corresponding to radioiodinated Ro 31–8472. Fractions of highest radioactivity were pooled, and 15 μl of 10 M NaOH were added per ml of ^{125}I-Ro 31–8472, to raise the pH to the range of subsequent radioligand binding studies. Aliquots of pH-adjusted ^{125}I-Ro 31–8472 and ^{125}I-351A were stored at −20° and were stable for up to 3 months.

Radioligand binding studies and data analysis. To duplicate tubes were added 250 μl of diluted plasma, tissue membrane preparation, or purified ACE and 50 μl of ^{125}I-Ro 31–8472 (40,000 cpm, 5 pg/tube) or ^{125}I-351A (40,000 cpm, 6 pg/tube). Dilutions were made in binding buffer (0.05 M Tris·HCl containing 0.3% BSA, 75 mM NaCl, 50 μM $ZnSO_4$, and 0.02% NaN_3, at pH 7.0). The final chloride concentration was 100 mM, after adjustment of the pH of the Tris buffer to pH 7.0 with HCl. Tubes were equilibrated at room temperature (20°) for 20 hr. Absolute ethanol (1 ml) was added, and the tubes were vortexed and then centrifuged (Beckman GPR, 1800 × *g* for 5 min). The supernatant was discarded, and the pellet, containing the ethanol-precipitated proteins and ACE-bound radioactivity, was counted in a γ counter (LKB 1260 Multigamma II).

Scatchard (14) and slope factor analyses were performed on binding displacement data obtained in the presence of concentrations of unlabeled Ro 31–8472, cilazaprilat, enalaprilat, lisinopril, and 351A over the range of 10^{-7} to 10^{-12} M. Studies were performed on two to five separate occasions. All data are expressed as mean ± standard error, and the number of binding sites was corrected per mg of protein (15). Iterative analysis and Scatchard analysis of data were performed with the LIGAND program of Munson and Rodbard (16), which calculated values for equilibrium dissociation constant (K_d) and density of binding sites (B_{max}) for each ACE sample, based on the goodness of fit for a one- or two-binding site model. Simultaneous fitting of families of sigmoidal displacement curves, to obtain slope factors, and comparison of slope factors among a panel of ACE inhibitors for plasma and tissue ACE were analyzed by the ALLFIT program of DeLean *et al.* (17). Hill coefficients (18) were calculated by linear regression analysis.

The time course for association of the ^{125}I-Ro 31–8472/ACE complex was established by incubating diluted plasma and radioligand for up to 24 hr, followed by ethanol separation. Dissociation of the radioligand/ACE complex was measured after the addition of 10^{-6} M unlabeled Ro 31–8472, preceded by 24 hr of preincubation with radioligand at room temperature. Subsequent ethanol separation was performed from 5 min to 19 hr after the addition of unlabeled 10^{-6} M Ro 31–8472. The association (k_{+1}) and dissociation (k_{-1}) constants for the ^{125}I-Ro 31–8472/plasma ACE complex were calculated by the KINETIC program of McPherson (19), which compared the goodness of fit for curves based on a one- or two-binding site model.

Tissue membrane ACE preparation. Male Sprague Dawley rats (200–250 g) were killed by decapitation, trunk blood was collected into a chilled heparin tube (500 IU/ml), and testes, kidneys, and whole lung were removed. Blood was centrifuged at 1800 × *g* for 15 min at 4°. Plasma and tissues were stored at −20° until required.

Membrane homogenates were prepared from thawed tissues by the method of Florentin *et al.* (20). Briefly, both testes, kidneys, and lungs were chopped very finely with a scalpel blade (1 mm^3), suspended in 12 ml of ice-cold binding buffer, homogenized (UltraTurrax T-25; Janke and Kunkel, Staufen, Germany) at 13,500 rpm for two bursts of 10 sec and filtered through two layers of cotton gauze, and the filtrate was centrifuged (Beckman, Irvine, CA) at 800 × *g* for 5 min at 4°. The supernatant was centrifuged at 60,000 × *g* for 60 min at 4° in a Beckman LM-8 ultracentrifuge with a SW30 rotor. Pellets were resuspended in binding buffer, homogenized manually using 10 strokes with a Teflon pestle in a ground glass tube, and brought to a total volume of 10 ml for each tissue. Plasma and tissue preparations were studied over a range of dilutions, to establish the protein concentration required for binding of approximately 10% of ^{125}I-Ro 31–8472 or ^{125}I-351A, at which subsequent experiments were performed.

Affinity purification of rat lung and testis ACE. The ACE inhibitor lisinopril was used to prepare an affinity column by the method of Hooper and Turner (21). The affinity gel contained a 2.8-nm spacer group between lisinopril and the Sepharose CL-4B (Pharmacia) matrix, to maximize the binding capacity of the affinity gel, as demonstrated by Pantoliano *et al.* (22).

The purification procedure was modified from that of Pantoliano *et al.* (22). Six whole lungs or testes were chopped, suspended in 25 ml of ice-cold binding buffer, homogenized, centrifuged, and ultracentrifuged as for the tissue ACE membrane preparation. Pellets were resuspended

in 30 ml of 10 mM sodium phosphate buffer, pH 7.8, and then homogenized manually for 10 stokes. ACE was solubilized from the membranes with a 5:1 (w/w) Triton X-100 to protein ratio, with mixing, for 2 hr at 4°. The suspension was centrifuged at 60,000 × *g* for 60 min at 4°, and the supernatant was dialyzed against 4 liters of 20 mM MES buffer, pH 6.0, containing 300 mM NaCl, 100 μM $ZnSO_4$, 0.02% NaN_3, and 890 mg/liter Triton X-100 (buffer A), at 4°. All affinity gel procedures were performed at room temperature. The dialyzed sample was applied, at 6 ml/hr, to the affinity column (gel volume, 25 ml; equilibrated in buffer A) and then washed with 130 ml of buffer A, followed by 400 ml of 20 mM MES buffer, pH 6.0, containing 300 mM NaCl and 0.02% NaN_3 (buffer B). Bound ACE was eluted from the affinity gel with 50 mM sodium borate, pH 8.9. Fractions containing ACE activity were pooled, vacuum dialyzed against 50 mM sodium phosphate buffer, pH 7.4, containing 0.02% NaN_3, and concentrated to a total volume of approximately 1 ml. Protein content was determined by the fluorescamine method of Udenfreid *et al.* (23), and ACE activity by the kinetic method of Friedland and Silverstein (10). Aliquots of purified ACE were stored at −20° until required.

Polyacrylamide gel electrophoresis, Western transfer, and radioligand binding analysis of purified ACE. Purified lung (25 ng) and testis (7 ng) ACE was electrophoresed (Mini-protean II dual slab cell; Bio-Rad, Richmond, CA) on a 7.5% polyacrylamide gel, under reducing conditions (2% sodium dodecyl sulfate, 2-mercaptoethanol), and was stained for protein by using a Bio-Rad silver stain kit.

Purified lung and testis ACE was electrophoresed on a native 7.5% polyacrylamide gel (without sodium dodecyl sulfate or 2-mercaptoethanol). Western transfer onto nitrocellulose (0.45-μm; Bio-Rad) was performed by overnight electrophoretic transfer at 20 V, 40 mA, in 25 mM Tris, 192 mM glycine, at pH 8.3 (Bio-Rad Mini Trans-Blot). Lung and testis ACE bound to nitrocellulose was washed overnight with 2% BSA at 4°, followed by binding buffer at room temperature, and was incubated with either ^{125}I-Ro 31–8472 or ^{125}I-351A (0.55 μCi/ml), in binding buffer containing 0.05% Tween 20. Constant mixing was maintained for the 3-hr incubation at room temperature. Nonspecific binding was assessed in the presence of either 1 mM EDTA or 10^{-6} M unlabeled Ro 31–8472. Excess unbound radioligand was removed from the nitrocellulose by four successive 3-min washes in binding buffer at 0°. Membranes were air dried, placed in X-ray cassettes under plastic, and exposed to Agfa Scopix CR3 X-ray film (Agfa-Gevaert, Melbourne, Australia) for 72 hr. The X-ray films were processed in a Kodak RPX-OMAT automatic developer (Rochester, NY).

Autoradiographic localization of radioligand binding to kidney ACE. For autoradiography using ^{125}I-Ro 31–8472 or ^{125}I-351A, a procedure published previously for ^{125}I-351A was used (24). Male Sprague-Dawley rats were killed by decapitation, and kidneys were removed and rapidly frozen in isopentane at −40°. Kidney sections were cut at 20 μm in a −20° cryostat. Sections were thaw mounted onto gelatin-coated slides and dried in a desiccator for 2 hr at 4°. The sections were preincubated in 10 mM phosphate buffer containing 150 mM NaCl and 0.2% BSA, pH 7.4, for 15 min at 20°, and then were incubated in buffer containing 0.3 μCi/ml ^{125}I-Ro 31–8472 or ^{125}I-351A, for 1 hr at 20°. Nonspecific binding was determined in parallel incubations containing 10^{-6} M Ro 31–8472 or 351A. After incubation, the sections were transferred through four successive 1-min washes of buffer without BSA, at 0°. The slides were dried under a stream of cold air, loaded into X-ray cassettes, and exposed to Agfa Scopix CR3 X-ray film (Agfa-Gevaert) for 24 hr. The X-ray films were processed in a Kodak RPX-OMAT automatic developer, and the optical density was quantitated using an EyeCom model 850 image analysis system (Spatial Data Systems, Springfield, VA) coupled to a DEC 11/23 LSI computer.

Statistical analysis. Comparisons between lung, kidney, testis, and plasma ACE for LIGAND parameters of K_d and B_{max} were by unpaired Student's *t* test. ALLFIT parameter of slope factor for the panel of ACE inhibitors using plasma, lung, kidney, or testis ACE were compared by constraining (sharing) slope factors. The goodness of fit was evaluated by the "extra sum of squares principle" and compared for unconstrained and constrained slope factors, which gave an *F* test value. Correlation coefficients were estimated by linear regression analysis, using the least squares method. $p < 0.05$ was required for significance.

Results

Relative ACE Enzymatic Inhibitory Potency of ACE Inhibitors

Ro 31–8472, cilazaprilat, lisinopril, enalaprilat, and 351A reduced ACE enzymatic activity in a dose-dependent manner. The calculated IC_{50} values are shown in Fig. 1 for each of the inhibitors.

Ligand Integrity and Stability

The high performance liquid chromatography elution profile of Ro 31–8472 contained a reproducible single peak, 10.2 min after sample injection.

Binding of ^{125}I-Ro 31–8472 to tissue and plasma ACE preparations rapidly reached equilibrium, with an estimated $t_{1/2}$ of association of 5 min. Binding remained constant over the 24-hr incubation period at 20° (Fig. 2). Unlabeled Ro 31–8472 at 10^{-6} M rapidly displaced ^{125}I-Ro 31–8472 from ACE, with an estimated $t_{1/2}$ of dissociation of 20 min. Resultant nonspecific binding was <1% of total binding. Binding of ^{125}I-Ro 31–8472 was proportional to the protein concentration of purified ACE, tissue membrane, or plasma and attained a maximal specific binding of 80% of added radioligand. The association (k_{+1}) and dissociation (k_{-1}) constants for ^{125}I-Ro 31–8472 interaction with plasma ACE were best fitted by a biexponential model (k_{+1}: first site, 9.7×10^9 M^{-1} min^{-1}; second site, 4.1×10^8 M^{-1} min^{-1}; $F = 4.8$; $p < 0.05$; k_{-1}: first site, 4.9×10^{-3} min^{-1}; second site, 2.7×10^{-2} min^{-1}; $F = 178$; $p < 0.001$, compared with a monoex-

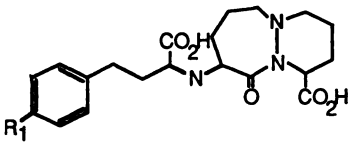

Cilazaprilat : R_1 = H IC_{50} = 0.7 nM

Ro 31-8472 : R_1 = OH IC_{50} = 0.6 nM

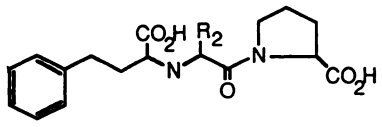

Enalaprilat : R_2 = CH_3 IC_{50} = 3.5 nM

Lisinopril : R_2 = $(CH_2)_4NH_2$ IC_{50} = 1.9 nM

351A : R_2 = $(CH_2)_4NHC(NH)$ 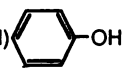

 IC_{50} = 1.4 nM

Fig. 1. Chemical structure and respective inhibitory potency (IC_{50}), as assessed by an enzyme kinetic method, for the bicyclic ACE inhibitors cilazapril and Ro 31–8472 (*upper*) and the monocyclic ACE inhibitors enalaprilat, lisinopril, and 351A (*lower*).

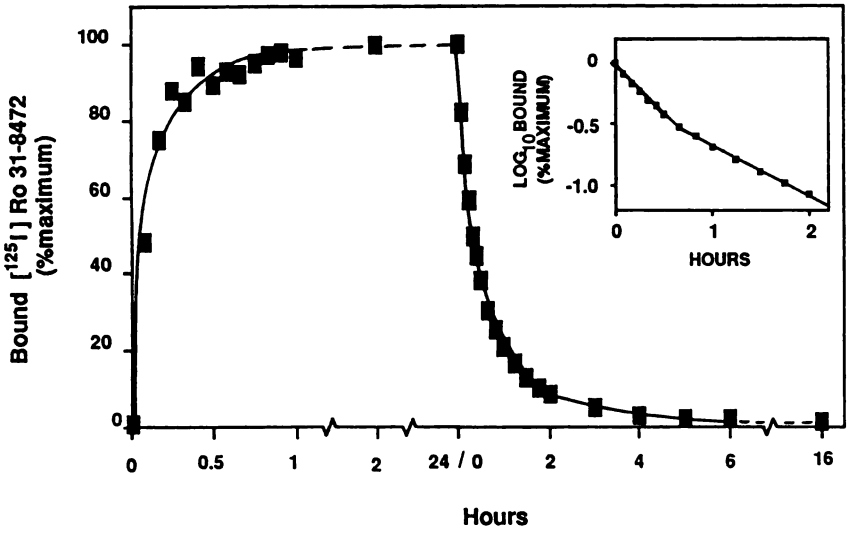

Fig. 2. Time course for association, followed by dissociation (started by addition of 10^{-6} M unlabeled Ro 31–8472), of the plasma ACE/^{125}I-Ro 31–8472 complex. *Inset*, logarithmic plot of ^{125}I-Ro 31–8472 dissociation from plasma ACE. The association and dissociation constants for ^{125}I-Ro 31–8472 interaction with plasma ACE were best fitted by a biexponential model. Dissociation of radioligand appeared to be biphasic, with calculated equillibrium dissociation constants (K_d), from predicted values of k_{+1} and k_{-1}, of 52.5 pM and 66.8 pM for the predicted carboxyl- and amino-terminal binding sites, respectively.

ponential fit). Logarithmic transformation of ^{125}I-Ro 31–8472 dissociation from plasma ACE is shown in Fig. 2. Dissociation of radioligand appeared to be biphasic, as confirmed by KINETIC analysis. The equilibrium dissociation constant (K_d) for ^{125}I-Ro 31–8472 calculated from the KINETIC parameter values of k_{+1} and k_{-1} was 52.5 pM and 66.8 pM for the carboxyl- and amino-terminal binding sites, respectively.

Polyacrylamide Gel Electrophoresis and Radioligand Binding to Purified ACE

Purified ACE migrated as a single protein band, which corresponded to a molecular mass of 150 kDa and 110 kDa for lung and testis ACE, respectively. Electrophoresis before Western blotting was performed under native conditions, to retain ACE binding activity. After native polyacrylamide gel electrophoresis and subsequent Western transfer, both ^{125}I-Ro 31–8472 and ^{125}I-351A bound to a single protein band, of higher or lower molecular weight for purified lung or testis ACE, respectively. Binding of both radioligands also occurred in the region corresponding to the interface between the spacer and running gels. This radioligand binding represented aggregates of purified ACE, which form under nonreducing conditions. Binding of either radioligand was completely displaced by 10^{-6} M unlabeled Ro 31–8472 or 1 mM EDTA.

Autoradiographic Localization of Kidney ACE

The regional distribution of ^{125}I-Ro 31–8472 and ^{125}I-351A binding to sections of kidney ACE was identical, indicating that these radioligands bound to the same protein. The highest density of radioligand binding occurred on the inner cortex (Fig. 3), corresponding to the reported ACE localization in the brush border of proximal tubules.

Radioligand Displacement Curves and Slope Factors

Displacement of ^{125}I-Ro 31–8472 from membrane sources, plasma, and purified lung and testis ACE by Ro 31–8472, cilazaprilat, enalaprilat, lisinopril, and 351A was concentration dependent (Fig. 4). ALLFIT analysis of displacement curves revealed significant differences in slope factors for lung, kidney, and plasma ACE, across the panel of ACE inhibitors studied. A direct linear correlation between the Hill coefficient and slope factor was found ($r = 0.95$; $y = 1.17x - 0.13$; 54 determinations; $p < 0.001$). Slope factors and Hill coefficients approximated 1.0 for testicular ACE (Table 1). The reduction in slope factor for lung, kidney, and plasma was related to the side chain size of the competing unlabeled ACE inhibitor (Fig. 1) and suggested displacement of ^{125}I-Ro 31–8472 from more than one population of ligand binding sites.

Quantitation of Binding Sites and Equilibrium Dissociation Constants

Membrane and plasma ACE. Representative Scatchard plots for ^{125}I-Ro 31–8472 displacement by 351A are shown in Fig. 5. Curves for plasma, lung, and kidney ACE were best fitted by a two-binding site model with shared binding site number (B_{max}) at the carboxyl- and amino-terminal binding sites. Model fitting for radioligand binding data for plasma, lung, and kidney ACE showed a marked improvement in the sum of squares, runs test, and plot of residuals for a two-binding site fit, compared with a one-binding site fit, with computed F values in excess of 55 (Table 2). CV for K_d and B_{max} ranged from 5% to 17% and 1% to 8%, respectively. In analyses where the binding site number was not constrained, the LIGAND program indicated that the model was poorly determined or predicted parameter values with excessively high CV (>50%). Testicular ACE bound ^{125}I-Ro 31–8472 at one site ($F = 0.8$; $p > 0.05$, compared with a two-site fit), with CV of 8–16% and 3–7% for K_d and B_{max}, respectively. The relative concentration of ACE binding sites for each tissue and plasma (Table 2) displayed the same rank order as that reported for ACE enzymatic activities and binding site numbers using other radioligands (25, 26). K_d values for Ro 31–8472 at the carboxyl- and amino-terminal binding sites were equimolar for plasma, lung, and kidney ACE (Table 2), in agreement with K_d values for plasma ACE obtained by KINETIC analysis. The affinity of 351A at the carboxyl- and amino-terminal binding sites differed by 65–210-fold for somatic ACE. Testicular ACE resembled plasma, lung, and kidney ACE at the carboxyl-terminal site only (Table 2), with similar K_d values for Ro 31–8472 and 351A. There were no significant differences in K_d with Ro 31–8472 or 351A, at a given binding site, for plasma and the tissue ACE sources studied.

Purified ACE. For purified testis and lung ACE, LIGAND analysis of ^{125}I-Ro 31–8472 displacement by 351A was best fitted by a one- and two-binding site model, respectively. The 351A K_d for the carboxyl- and amino-terminal binding sites of

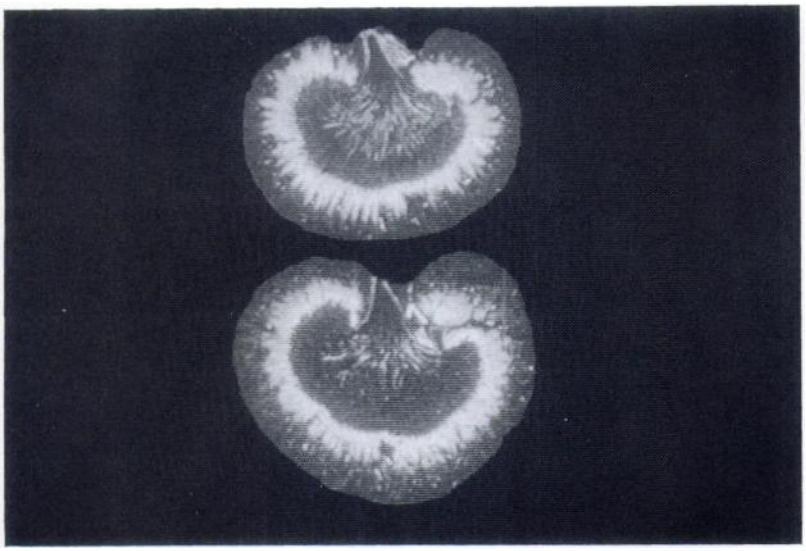

Fig. 3. Autoradiographic localization of kidney ACE, using ^{125}I-Ro 31–8472 (*upper kidney*) and ^{125}I-351A (*lower kidney*). The two radioligands bound to kidney ACE with very similar distributions, with highest binding density corresponding to the collecting tubules of the inner cortex.

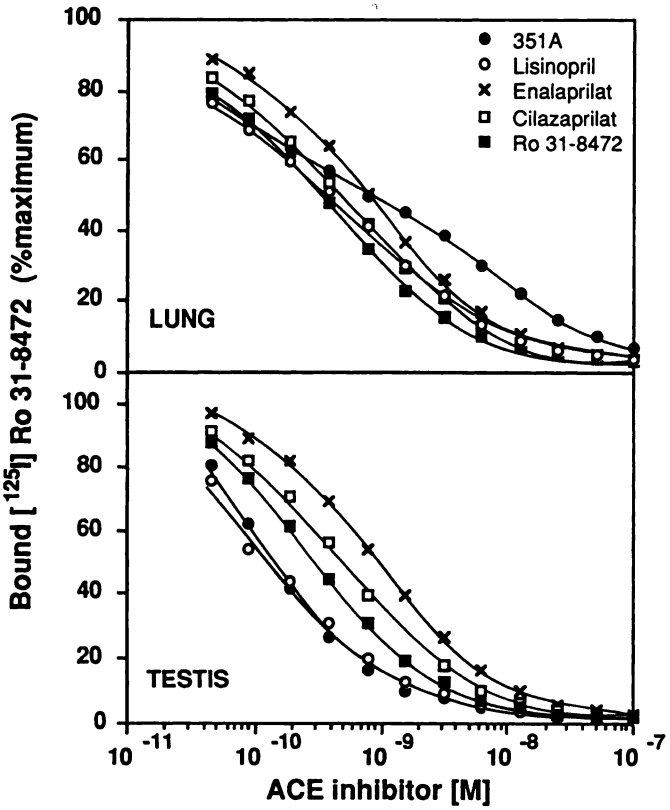

Fig. 4. Displacement of ^{125}I-Ro 31–8472 binding from lung ACE (*upper*) and testis ACE (*lower*) by increasing concentrations of 351A (●), lisinopril (○), enalaprilat (×), cilazaprilat (□), or Ro 31–8472 (■). Binding displacement curves from lung ACE showed varying degrees of nonparallelism across the ACE inhibitors studied. Model fitting for radioligand binding displacement data best fitted a two-binding site model. In contrast, displacement curves with testicular ACE were of similar configuration, and analysis of binding displacement data best fitted a one-binding site model.

purified lung ACE were similar to those for somatic membrane and plasma ACE (Tables 2 and 3). The binding affinities for 351A at the two binding sites differed by 140-fold for purified lung ACE, in agreement with the 140–210-fold difference in binding affinities for somatic membrane ACE (Tables 2 and 3). The K_d of 351A at the single testis ACE binding site resembled that at the carboxyl-terminal binding site of purified lung ACE (Table 3).

Displacement of ^{125}I-351A by unlabeled 351A or Ro 31–8472 occurred at a single binding site for purified lung and testis ACE. The magnitude of K_d for 351A and Ro 31–8472 was significantly lower using ^{125}I-351A than ^{125}I-Ro 31–8472 (Table 3). However, the rank order of binding affinities for Ro 31–8472 and 351A at the single lung or testis ACE binding site obtained using the ^{125}I-351A radioligand was identical to the rank order of carboxyl-terminal binding site affinities for these unlabeled ACE inhibitors obtained in ^{125}I-Ro 31–8472 studies.

Discussion

Molecular biology studies of human and mouse ACE RNA predict the existence of two active sites in the ~150-kDa ACE protein of somatic cell origin and one active site in the ~100-kDa ACE protein of testicular origin (6–9). The testicular ACE protein predicted from the RNA sequence corresponds to the carboxyl-terminal region of somatic ACE and contains one of the two homologous active site-bearing domains found in somatic ACE (8, 9). Expression of the amino- or carboxyl-terminal portion of the ACE protein by a cell culture system (after insertion of the relevant DNA segment) has yielded two proteins, each able to cleave synthetic substrates for ACE or the natural ACE substrate angiotensin I. The amino-terminal portion of ACE produced by the transfected cells has been shown to be less active than the carboxyl-terminal portion of ACE, with differences in sensitivity to chloride ion activation (27). The tertiary structure of these cloned fragments of ACE may differ from the full length "wild-type" (glycosylated) molecule. The enzymatic characteristics of some, but not all, membrane associated-enzymes are known to be altered by detergent solubilization of the enzyme from the cell membrane (28). Similarly, detergent solubilization of receptors has been shown to change the affinity of membrane receptors for ligands (29). Our ^{125}I-Ro 31–8472 binding studies showed that the presence or absence of the cell membrane associated with tissue ACE, or the absence of the cell membrane and carboxyl-terminal hydrophobic anchor region on plasma ACE, did not influence ACE inhibitor binding affinity at the carboxyl- and amino-terminal binding sites.

TABLE 1

Slope factors for ^{125}I-Ro 31-8472 displacement from plasma, lung, kidney, and testis ACE by a panel of five ACE inhibitors

Results are the mean ± standard error, with the number of determinations shown in parentheses. The reduction in slope factor for lung, kidney, and plasma was related to the side chain size of the competing unlabeled ACE inhibitor and suggested that displacement of ^{125}I-Ro 31-8472 was from more than one population of ligand binding sites. In contrast, slope factors for testis ACE approximated 1.0, suggesting that displacement was from one population of ligand binding sites in ACE from testis.

ACE source	Slope factor				
	Ro 31-8472	Cilazaprilat	Enalaprilat	Lisinopril	351A
Plasma	0.83 ± 0.02 (5)	0.78 ± 0.05 (2)	0.81 ± 0.03 (2)	0.56 ± 0.02 (2)[a]	0.41 ± 0.07 (5)[a]
Lung	0.82 ± 0.03 (5)	0.87 ± 0.03 (2)	0.91 ± 0.02 (2)	0.66 ± 0.08 (2)[a]	0.38 ± 0.04 (5)[a]
Kidney	0.84 ± 0.02 (3)	ND[b]	ND	ND	0.38 ± 0.04 (3)[a]
Testis	0.93 ± 0.02 (5)	0.91 ± 0.01 (2)	0.91 ± 0.01 (2)	0.87 ± 0.03 (2)[c]	0.96 ± 0.04 (5)

[a] $25.9 < F < 70.1$; $p < 0.001$.
[b] ND, not determined.
[c] $F = 2.6$; $p < 0.01$.

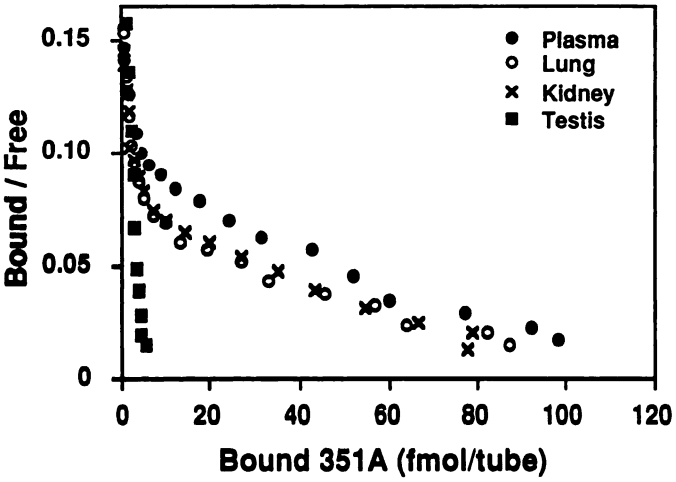

Fig. 5. Scatchard plot for displacement of ^{125}I-Ro 31-8472 binding from plasma (●), lung (○), kidney (×), and testis (■) ACE by increasing concentrations of 351A. Data for plasma lung and kidney best fitted a two-binding site model, whereas binding displacement data for testicular ACE best fitted a one-binding site model.

TABLE 2

Binding parameters (K_d and B_{max}) for Ro 31-8472 and 351A displacement of ^{125}I-Ro 31-8472 from rat plasma ACE and lung, kidney, and testis membrane ACE

K_{d_1} and K_{d_2} indicate the K_d values at the carboxyl- and amino-terminal binding sites respectively. B_{max} represents the total number of binding sites per mg of plasma or tissue protein. Results are the mean ± standard error for triplicate determinations. K_d values at the carboxyl- and amino-terminal binding sites in plasma lung and kidney were similar for Ro 31-8472 but were clearly different for 351A.

ACE source	Displacement by Ro 31-8472		Displacement by 351A		B_{max}
	K_{d_1}	K_{d_2}	K_{d_1}	K_{d_2}	
	pM		pM		pmol of Ro 31-8472/mg of protein
Plasma[a]	142 ± 33	175 ± 38	41 ± 14	2679 ± 385[bc]	0.64 ± 0.13
Lung[a]	94 ± 33	114 ± 39	13 ± 4	2738 ± 223[bc]	29.15 ± 9.59
Kidney[a]	104 ± 31	75 ± 19	18 ± 4	2604 ± 612[bc]	1.11 ± 0.53
Testis[d]	54 ± 15		26 ± 8		7.46 ± 2.86

[a] $55.3 < F < 242.5$; $p < 0.001$, compared with a one-site fit.
[b] $p < 0.01$, compared with the Ro 31-8472 K_{d_1}.
[c] $p < 0.01$, compared with the 351A K_{d_1}.
[d] $F = 0.8$; $p > 0.05$.

Activation by chloride ion of ACE from numerous sources and species has been demonstrated by kinetic enzymatic studies, using natural (30) or synthetic (10) substrates. Chloride ion interacts with a critical lysine residue at or near the active site, to activate ACE (31), and enhances isomerization of the enzyme/inhibitor complex to a more tightly bound form (32).

TABLE 3

Binding parameters of K_d for Ro 31-8472 and 351A displacement of ^{125}I-Ro 31-8472 and ^{125}I-351A from purified rat lung and testis ACE

K_{d_1} and K_{d_2} indicate the K_d values at the carboxyl- and amino-terminal binding sites, respectively. Results are the mean ± standard error for triplicate determinations. ^{125}I-Ro 31-8472 was displaced from two binding sites on lung ACE. K_d values at the carboxyl- and amino-terminal binding sites for lung ACE were similar for Ro 31-8472 but were clearly different for 351A. ^{125}I-351A was displaced from a single binding site on lung and testis ACE, the K_d of which resembled the carboxyl-terminal binding site affinities from ^{125}I-Ro 31-8472 displacement studies.

ACE source	^{125}I-Ro 31-8472 displacement by				^{125}I-351A displacement by	
	Ro 31-8472		351A		Ro 31-8472, K_{d_1}	351A K_{d_1}
	K_{d_1}	K_{d_2}	K_{d_1}	K_{d_2}		
	pM				pM	
Lung[a]	65 ± 7	175 ± 38	19 ± 2	2771 ± 489[bc]	32 ± 7[d]	15 ± 3
Testis	46 ± 6		16 ± 3		19 ± 3[d]	6 ± 2[d]

[a] $15.4 < F < 104.3$; $p < 0.001$, compared with a one-site fit, for ^{125}I-Ro 31-8472 studies.
[b] $p < 0.01$, compared with the Ro 31-8472 K_{d_1} from ^{125}I-Ro 31-8472 studies.
[c] $p < 0.01$, compared with the 351A K_{d_1} from ^{125}I-Ro 31-8472 studies.
[d] $p < 0.05$, ^{125}I-Ro 31-8472 versus ^{125}I-351A studies.

Dissociation of the ACE/ACE inhibitor complex is greatly increased by chloride-free conditions (33). In preliminary studies, binding of ^{125}I-Ro 31-8472 to ACE was shown to be chloride ion dependent, with optimal binding over the range of 100–250 mM chloride. All binding experiments in this study were performed using 100 mM chloride ion. The effect of varying the chloride ion concentration on the interaction of ACE inhibitors or substrates with the ACE active site(s) was not assessed in this study but warrants investigation.

Radioligand binding studies using ^{125}I-Ro 31-8472 and ACE of plasma or tissue origin, in the current report, support the existence of two binding sites in ACE from lung, kidney, and plasma and one binding site in testis ACE. This is the first confirmation that circulating and membrane-bound somatic ACE in the intact native form possess two functional binding sites. In agreement with molecular biology studies, the single testicular ACE binding site resembles one of the two sites of somatic ACE, with equivalent K_d values for Ro 31-8472 or 351A at the carboxyl-terminal binding site. The second binding site, in the amino-terminal half of somatic cell ACE, which has been reported to be of 3- or 9-fold lower enzymatic activity in the presence of natural or synthetic substrates, respectively (27), was demonstrated in ligand binding studies of ACE from lung, kidney, and plasma to possess a K_d for 351A from 65- to 210-fold higher than that at the carboxyl-terminal binding site.

Previous radioligand binding studies with [^{3}H]RU 44-403 (33), [^{3}H]captopril (34), [^{3}H]enalaprilat (35), and ^{125}I-351A (26)

have all reported the presence of one population of binding sites for somatic ACE, despite the suggestions from RNA analysis. Wei *et al.* (27) noted that cloned fragments of the amino-terminal ACE fragment bound poorly to a lisinopril-coupled affinity column, consistent with the suggestion that the binding affinity of lisinopril was reduced at the amino-terminal putative enzymatic site (see Table 1 and Fig. 4). Stochiometric analysis of ACE inhibitor interaction with purified lung and kidney ACE has revealed binding of 2 mol of lisinopril/mol of ACE protein. The binding affinity of lisinopril at the amino-terminal binding site was reduced but not formally quantitated (36). Our studies suggest that the K_d for 351A, a derivative of lisinopril, at the amino-terminal binding site of ACE is some 2 orders of magnitude higher than that at the carboxyl-terminal binding site. The low affinity of 351A at the amino-terminal binding site would make the detection of a second binding site by using side chain-substituted radioligands, such as 351A or lisinopril, difficult. This is supported by our radioligand binding studies of ^{125}I-351A or ^{125}I-Ro 31–8472 displacement from purified rat lung ACE by 351A, which occurred at one and two binding sites, respectively.

Purification of ACE by affinity chromatography techniques, utilizing ligands such as lisinopril (36, 37), *N*-[1(*S*)-carboxy-5-amino-pentyl]-L-Phe-Gly, or *N*-[1(*S*)-carboxy-5-amino-pentyl]-DL-alanyl-L-proline (38), reveals that the binding capacity of affinity supports for ACE is directly proportional to the length of the spacer arm between the support matrix and the immobilized ligand. For full binding affinity of ACE to the affinity gel, a spacer arm in excess of 20 Å is required (37, 38); therefore, the active site of ACE appears to be deeply recessed, rather than located on the surface of the protein. With reduced spacer arm length, steric hindrance contributed to the reduced binding capacity of affinity chromatographic media.

In this study, the slope factors for Ro 31–8472, cilazaprilat, and enalaprilat displacement of ^{125}I-Ro 31–8472 binding from plasma or lung ACE were significantly closer to 1 than slope factors for lisinopril and 351A, whereas studies using testicular ACE were not influenced by the structure of the displacing unlabeled ACE inhibitor. Unlike the bicyclic ACE inhibitors cilazaprilat and Ro 31–8472, the inhibitors enalaprilat, lisinopril, and 351A possess side chains of increasing length. 351A is a *p*-hydroxybenzamidine derivative of lisinopril, which is, in turn, the Lys-Pro analogue of enalaprilat. These ACE inhibitors, with increasing side chain length, may encounter steric hindrance at the deeply recessed ACE active site in the somatic ACE form. This was particularly pronounced at the amino-terminal binding site of somatic ACE in our studies. Despite differences in catalytic activity, the K_m of the carboxyl- and amino-terminal active sites was shown to be similar with either angiotensin I or hippuryl-histidyl-leucine (27). The side chains on the amino acids for these two substrates are minor, compared with those for lisinopril and 351A, and presumably these substrates encounter minimal steric hindrance at the amino-terminal active site. In our studies, displacement of radioligand from testicular ACE was not influenced by the structure of the displacing unlabeled ACE inhibitor, which corresponds to observations at the carboxyl-terminal binding site in somatic ACE. These observations suggest that there are differences in the accessibility to ACE inhibitors for the two active sites of somatic ACE, with the amino-terminal binding site being more sensitive to the structure of the ACE inhibitor than is the carboxyl-terminal binding site. Differential steric hindrance by inhibitors or natural substrates in the deeply recessed active site(s) may play a role in regulating or restricting substrate interaction with ACE. Despite the presence of two active sites on somatic ACE and one active site on testicular ACE, the catalytic activity of the intact somatic enzyme is similar to that of the testicular enzyme with natural or synthetic substrates. The function of this second site is largely unknown. Studies by Ehlers and Riordan (36) have shown the aminotripeptidase and carboxytripeptidase cleavage of gonadotrophin-releasing hormone by ACE may predominate at the amino-terminal active site of ACE.

The amino acid sequences for the carboxyl- and amino-terminal halves of the somatic ACE molecule are >60% homologous and share 89% homology for regions comprising the putative active sites (6). However, the substrate specificity for the two active sites may differ, as indicated by our binding studies. CPA2 has been shown to display unique substrate specificity for tryptophan terminal substrates, compared with CPA1, yet CPA2 arose from gene duplication and shares 63% amino acid sequence homology with CPA1 (39). Studies comparing the structure of bovine CPA1 and rat CPA2 have revealed two amino acid substitutions in the binding cavity, only one of which is in direct contact with substrate (40). The enlarged active site region of CPA2, compared with CPA1 (required to accommodate larger amino acids, such as tryptophan), appeared to be related to replacement of Thr^{268} with alanine and differences in the structure of the active site surface loop. Conserved amino acid sequences of the active site surface loop between CPA2 and CPA1 also differed in the orientation of binding residues. Both enzymes contained Tyr^{248} at the active site surface loop, but only in the case of CPA2 was this amino acid located in the specificity pocket to block substrate access to the active site. Similar subtle differences in structure between the amino- and carboxyl-terminal halves of the somatic ACE molecule may also influence and regulate substrate specificity.

Binding of radioligand to membrane preparations may have identified two separate proteins, rather than two regions of the one protein. This possibility has been addressed by studies of highly purified ACE. Ligand-binding characteristics were similar for purified ACE and membrane ACE. Furthermore, autoradiography of radioligand binding to Western blots showed precise co-localization of the two index radioligands to the same protein band, clearly confirming that binding of both radioprobes to purified lung and testis ACE was to one molecular species. Autoradiographic studies of radioligand binding to frozen tissue sections confirmed the Western blot results, by demonstrating the same regional localization of ACE in the kidney with both radioprobes. Our radioligand binding studies with ^{125}I-Ro 31–8472 have revealed two distinct, functional, binding sites in ACE from lung, kidney, and plasma of the rat. In contrast, testicular ACE possesses only one high affinity binding site, which resembles the carboxyl-terminal binding site delineated in somatic and circulating ACE. The presence of the cell membrane and hydrophobic carboxyl-terminal anchor zone on ACE did not influence the ACE inhibitor binding affinities at the two somatic ACE binding sites. Displacement of radioligand by different classes of ACE inhibitors suggests steric hindrance at the amino-terminal binding site for ACE of circulating and somatic cell origin. This was not seen in ACE

of testicular origin. Differential steric hindrance may influence accessibility and alter competition among natural substrates, or ACE inhibitors, at the ACE active site(s) and may regulate the specificity and activity of ACE.

References

1. Soffer, R. L. Angiotensin-converting enzyme and the regulation of vasoactive peptides. *Annu. Rev. Biochem.* **45**:73–94 (1976).
2. Skidgel, R. A., and E. G. Erdös. The broad substrate specificity of human angiotensin I converting enzyme. *Clin. Exp. Hypertens.* **9**:243–259 (1987).
3. Johnston, C. I., and B. Jackson. Angiotensin converting enzyme inhibitors, in *Cardiovascular Drug Therapy* (S. Hunyor, ed.). Williams and Wilkins, Sydney, 206–214 (1987).
4. Lanzillo, J. J., and B. L. Fanburg. Angiotensin I converting enzyme from human plasma. *Biochemistry* **16**:5491–5495 (1977).
5. Velletri, P. A., D. R. Aquilano, E. Brunswick, C. H. Tsai-Morris, M. L. Dufau, and W. Lovenberg. Endocrinological control and cellular localization of rat testicular angiotensin-converting enzyme (EC 3.4.15.1). *Endocrinology* **116**:2516–2522 (1985).
6. Soubrier, F., F. Alhenc-Gelas, C. Hubert, J. Allegrini, M. John, G. Tregear, and P. Corvol. Two putative active centers in human angiotensin I converting enzyme revealed by molecular cloning. *Proc. Natl. Acad. Sci. USA* **85**:9386–9390 (1988).
7. Bernstein, K. E., B. M. Martin, A. S. Edwards, and E. A. Bernstein. Mouse angiotensin-converting enzyme is a protein composed of two homologous domains. *J. Biol. Chem.* **264**:11945–11951 (1989).
8. Ehlers, M. R., E. A. Fox, D. J. Strydom, and J. F. Riordan. Molecular cloning of human testicular angiotensin-converting enzyme: the testis isozyme is identical to the C-terminal half of endothelial angiotensin-converting enzyme. *Proc. Natl. Acad. Sci. USA* **86**:7741–7745 (1989).
9. Kumar, R. S., J. Kusari, S. Roy, R. L. Soff, and G. C. Sen. Structure of testicular angiotensin converting enzyme: a segmental isozyme. *J. Biol. Chem.* **264**:16754–16758 (1989).
10. Friedland, J., and E. Silverstein. A sensitive fluorimetric assay for serum angiotensin-converting enzyme. *Am. J. Clin. Pathol.* **66**:416–424 (1976).
11. Jackson, B., R. Cubela, and C. I. Johnston. Angiotensin converting enzyme inhibitors: measurement of relative inhibitory potency and serum drug levels by radioinhibitor binding displacement assay. *J. Cardiovasc. Pharmacol.* **9**:699–704 (1986).
12. Jackson, B., R. Cubela, and C. I. Johnston. Characterization of angiotensin converting enzyme from rat tissue by radioinhibitor binding studies. *Clin. Exp. Pharmacol. Physiol.* **13**:681–689 (1986).
13. Hunter, W. M., and F. C. Greenwood. Preparation of iodine 131 labelled human growth hormone of high specific activity. *Nature (Lond.)* **194**:495–496 (1962).
14. Scatchard, G. The attraction of proteins for small molecules and ions. *Ann. N. Y. Acad. Sci.* **51**:660–672 (1949).
15. Lowry, O. H., N. J. Rosebrough, A. L. Farr, and R. J. Randall. Protein measurement with the Folin phenol reagent. *J. Biol. Chem.* **193**:265–275 (1951).
16. Munson, P. J., and D. Rodbard. LIGAND: a versatile computerized approach for the characterization of ligand binding systems. *Anal. Biochem.* **107**:220–239 (1980).
17. DeLean, A., P. J. Munson, and D. Rodbard. Simultaneous analysis of families of sigmoidal dose-response curves: application to bioassay, radioligand assay, and physiological dose-response curves. *Am. J. Physiol.* **235**:E97–E102 (1978).
18. Hill, A. V. The possible effects of the aggregation of the molecules of haemoglobin on its dissociation curves. *J. Physiol. (Lond.)* **40**:iv–vii (1910).
19. McPherson, G. A. Analysis of radioligand binding experiments: a collection of computer programs for the IBM PC. *J. Pharmacol. Methods* **14**:213–228 (1985).
20. Florentin, D., A. Sassi, and B. P. Roques. A highly sensitive fluorometric assay for "enkephalinase," a neutral metalloendopeptidase that releases tyrosine-glycine-glycine from enkephalins. *Anal. Biochem.* **141**:62–69 (1984).
21. Hooper, N. M., and A. J. Turner. Isolation of two differentially glycosylated forms of peptidyl-dipeptidase A (angiotensin converting enzyme) from pig brain: a re-evaluation of their role in neuropeptide metabolism. *Biochem. J.* **241**:625–633 (1987).
22. Pantoliano, M. W., B. Holmquist, and J. F. Riordan. Affinity chromatographic purification of angiotensin converting enzyme. *Biochemistry* **23**:1037–1042 (1984).
23. Udenfried, S., S. Stein, P. Bohlen, W. Dairman, W. Leimgruber, and M. Weigele. Fluorescamine: a reagent for assay of amino acids, peptides, proteins and primary amines in the picomolar range. *Science (Washington D. C.)* **178**:871–872 (1972).
24. Mendelsohn, F. A. O. Localization of angiotensin converting enzyme in rat forebrain and other tissues by *in vitro* autoradiography using ^{125}I-labelled MK351A. *Clin. Exp. Pharmacol. Physiol.* **11**:431–436 (1986).
25. Cushman, D. W., and H. S. Cheung. Concentration of angiotensin-converting enzyme in tissues of the rat. *Biochim. Biophys. Acta* **250**:261–265 (1971).
26. Jackson, B., R. Cubela, and C. I. Johnston. Angiotensin converting enzyme (ACE) characterization by ^{125}I-MK351A binding studies of plasma and tissue ACE during variation of salt status in the rat. *J. Hypertens.* **4**:759–765 (1986).
27. Wei, L., F. Alhenc-Gelas, P. Corvol, and E. Clauser. The two homologous domains of human angiotensin I converting enzyme are both catalytically active. *J. Biol. Chem.* **266**:9002–9008 (1991).
28. Sugiyama, H., and J. P. Changeux. Interconversion between different states of affinity for acetylcholine of the cholinergic receptor protein from *Torpedo marmorata*. *Eur. J. Biochem.* **55**:505–515 (1975).
29. Warren, G. B., P. A. Toon, N. J. M. Birdsall, A. G. Lee, and J. C. Metcalfe. Reversible lipid titrations of the activity of pure adenosine tri-phosphatase lipid complexes. *Biochemistry* **13**:5501–5507 (1974).
30. Ehlers, M. R., and R. E. Kirsch. Catalysis of angiotensin I hydrolysis by human angiotensin-converting enzyme: effect of chloride and pH. *Biochemistry* **27**:5538–5544 (1988).
31. Bünning, P., B. Holmquist, and J. F. Riordan. Functional residues at the active site of angiotensin converting enzyme. *Biochem. Biophys. Res. Commun.* **83**:1442–1449 (1978).
32. Shapiro, R., and J. F. Riordan. Inhibition of angiotensin converting enzyme: dependence on chloride. *Biochemistry* **23**:5234–5240 (1984).
33. Cumin, F., V. Velland, P. Corvol, and F. Alhenc-Gelas. Evidence for a single active site in the human angiotensin I converting enzyme from inhibitor binding studies with RU44403: role of chloride. *Biochem. Biophys. Res. Commun.* **163**:718–725 (1989).
34. Strittmater, S. M., and S. H. Snyder. Characterization of angiotensin converting enzyme by [^{3}H]captopril binding. *Mol. Pharmacol.* **29**:142–148 (1986).
35. Bull, H. G., N. A. Thornberry, M. H. J. Cordes, A. A. Patchett, and E. H. Cordes. Inhibition of rabbit lung angiotensin-converting enzyme by *N*α-[(*S*)-1-carboxy-3-phenylpropyl]L-alanyl-L-proline and *N*α-[(*S*)-1-carboxy-3-phenylpropyl]L-lysyl-L-proline. *J. Biol. Chem.* **260**:2952–2962 (1985).
36. Ehlers, M. R. W., and J. F. Riordan. Angiotensin converting enzyme: zinc and inhibitor-binding stochiometries of somatic and testis isozymes. *Biochemistry* **30**:7118–7126 (1991).
37. Bernstein, K. E., B. M. Martin, L. Striker, and G. Striker. Partial protein sequence of mouse and bovine kidney angiotensin converting enzyme. *Kidney Int.* **33**:652–655 (1988).
38. Bernstein, K. E., S. L. Welsh, and J. K. Inman. A deeply recessed active site in angiotensin converting enzyme is indicated from the binding characteristics of biotin-spacer-inhibitor reagents. *Biochem. Biophys. Res. Commun.* **167**:310–316 (1990).
39. Gardell, S. J., C. S. Craik, E. Clauser, E. J. Goldsmith, C.-B. Stewart, M. Graf, and W. J. Rutter. A novel rat carboxypeptidase, CPA2: characterization, molecular cloning, and evolutionary implications on substrate specificity in the carboxypeptidase gene family. *J. Biol. Chem.* **263**:17828–17836 (1988).
40. Faming, Z., B. Kobe, C.-B. Stewart, W. J. Rutter, and E. J. Goldsmith. Structural evolution of an enzyme specificity: the structure of rat carboxypeptidase A2 at 1.9-Å resolution. *J. Biol. Chem.* **266**:24606–24612 (1991).

Send reprint requests to: Dr. Bruce Jackson, Department of Medicine, The University of Melbourne, Austin Hospital, Heidelberg, Victoria, Australia 3084.